EURASIAN JOURNAL OF MATHEMATICAL AND COMPUTER APPLICATIONS
ISSN 2306–6172
Volume 5, Issue 3 (2017) 15 – 43

DETERMINATION OF TIME-DEPENDENT COEFFICIENTS AND MULTIPLE FREE BOUNDARIES

Huntul M.J., Lesnic D.

Abstract A difficult inverse problem consisting of determining the time-dependent coefficients and multiple free boundaries, together with the temperature in the heat equation with Stefan condition and several-orders heat moment measurements is, for the first time, numerically solved. The time-dependent missing information matches up quantitatively with the time-dependent additional information that is supplied. Although the inverse problem has a unique local solution, this problem is still ill-posed since small errors in input data cause large errors in the output solution. For the numerical realization, the finite difference method with the Crank-Nicolson scheme combined with the Tikhonov regularization are employed in order to obtain an accurate and stable numerical solution. The resulting nonlinear minimization problem is computationally solved using the MATLAB toolbox routine *lsqnonlin*. A couple of numerical examples are presented and discussed to verify the accuracy and stability of the approximate solutions.

Key words: Inverse problem; Free boundaries; Heat equation; Tikhonov regularization.

AMS Mathematics Subject Classification: 65M32, 80A22.

1 Introduction

Free boundary problems involving Stefan condition have been considered to be one of the most important directions in the analysis of partial differential equations, with an abundance of applications to real world problems, including physics, chemistry, biology, [6], engineering, industry and other areas, [1, 4, 7]. For instance, during heat diffusion in melting ice, the boundary of the ice keeps on shifting, [11], and the latent heat is absorbed or released by the thermodynamic system without a change in temperature, [3]. In [2], the authors have discussed free boundary problems arising in two new scenarios, nonlocal diffusion and aggregation processes. The challenge of free boundary problems lies in the fact that the solution domain is unknown and has to be determined.

Determination of time-dependent coefficients problems involving free boundaries have been the point of interest of some recent works by Snitko [16, 17, 19]. In addition, in [15], the author investigated the parabolic heat equation with an unknown heat source and with a known moving boundary.

Inverse coefficient determination problems with one or several unknown coefficients play a substantial role in the theory and application of inverse problems. Using a simple change of variables, free boundary problems can be reduced to inverse coefficient problems in a fixed domain. In [9], we have investigated the inverse problems of simultaneous numerical reconstruction of time-dependent thermal conductivity/convection/absorption coefficient from heat moments. The finite difference method

(FDM) and regularized nonlinear optimization have been applied in order to obtain accurate and stable results.

In recent papers, [10, 11], the authors have investigated the determination of multiple time-dependent coefficients together with an unknown one side free boundary of the finite slab $0 < x < h(t)$. In this paper, we extend these analyses and investigate the determination of time-dependent coefficients together with two unknown free boundaries of the finite slab $h_1(t) < x < h_2(t)$. The inverse problems investigated in this paper have already been proved to be locally uniquely solvable by Snitko [18, 20], but no reconstruction has been attempted, and it is the aim of this paper to undertake the numerical solution of these problems.

The organization of the paper is as follows. The mathematical statements of the inverse problems are described in Section 2. In Section 3, the solution of the direct problem based on the FDM with the Crank-Nicolson scheme is presented. Since the inverse problem is ill-posed (in the sense that the continuous dependence upon the input data is violated), the numerical method based on the FDM direct solver is combined with the Tikhonov regularization method, as described in Section 4. In Section 5, numerical results for a couple examples are presented and discussed. Finally, conclusions are highlighted in Section 6.

2 Statements of the inverse problem

In the moving domain $\Omega_T = \{(x,t)|\ h_1(t) < x < h_2(t),\ 0 < t < T\}$, see Figure 1, where $h_1(t) < h_2(t)$ are unknown free boundaries, with unknown temperature $u(x,t)$ and unknown time-dependent coefficients $b_1(t)$ and $b_2(t)$, we consider solving the one-dimensional time-dependent parabolic equation given by

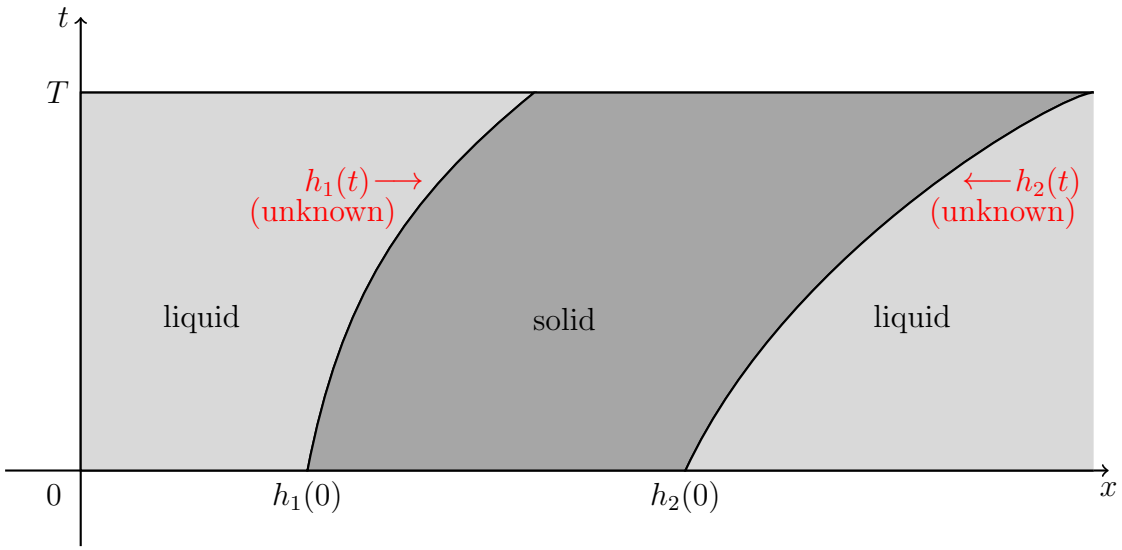

Figure 1: Sketch of the three-phase Stefan problem, with two unknown moving boundaries $h_1(t)$ and $h_2(t)$.

$$\frac{\partial u}{\partial t}(x,t) = a(x,t)\frac{\partial^2 u}{\partial x^2}(x,t) + (b_1(t)x + b_2(t))\frac{\partial u}{\partial x}(x,t) + c(x,t)u(x,t) + f(x,t), \quad (x,t) \in \Omega_T, \tag{1}$$

where $a > 0$ is the given thermal diffusivity, f is a given heat source and c is a given reaction rate, subject to the initial condition

$$u(x,0) = \varphi(x), \quad x \in [h_1(0), h_2(0)], \tag{2}$$

where $h_1(0) = h_{01}$ and $h_2(0) = h_{02}$ are given numbers satisfying $h_{01} < h_{02}$, the Dirichlet boundary conditions

$$u(h_1(t),t) = \mu_1(t), \quad u(h_2(t),t) = \mu_2(t), \quad t \in [0,T], \tag{3}$$

and the over-determination conditions

$$h_1'(t) - u_x(h_1(t),t) = \mu_3(t), \quad t \in [0,T], \tag{4}$$

$$h_2'(t) + u_x(h_2(t),t) = \mu_4(t), \quad t \in [0,T], \tag{5}$$

$$\int_{h_1(t)}^{h_2(t)} u(x,t)dx = \mu_5(t), \quad t \in [0,T], \tag{6}$$

$$\int_{h_1(t)}^{h_2(t)} xu(x,t)dx = \mu_6(t), \quad t \in [0,T], \tag{7}$$

where $\varphi(x)$ and $\mu_i(t)$ for $i = \overline{1,6}$ are given functions satisfying compatibility conditions.

Note that the equations (4) and (5) represent Stefan conditions of melting between a solid and liquid. Also, equations (6) and (7) represents the mass (energy) and the first-order heat moment, respectively. The term $b_1(t)x + b_2(t)$ in (1) represents a convective fluid velocity which is linear in x with unknown time-dependent coefficients $b_1(t)$ and $b_2(t)$.

The inverse problem is concerned with the invertibility of the map $(\mu_3, \mu_4, \mu_5, \mu_6) \mapsto (h_1, h_2, b_1, b_2)$.

Introducing the new variable $y = \frac{x - h_1(t)}{h_2(t) - h_1(t)}$, we recast the problem (1)–(7) into the following inverse problem for the unknowns $(h_1(t),\ h_3(t),\ b_1(t),\ b_2(t), v(y,t))$,
where $h_3(t) := h_2(t) - h_1(t)$ and $v(y,t) := u(yh_3(t) + h_1(t), t)$, see [18],

$$\begin{aligned}\frac{\partial v}{\partial t}(y,t) &= \frac{a(yh_3(t) + h_1(t), t)}{h_3^2(t)}\frac{\partial^2 v}{\partial y^2}(y,t) \\ &+\Big(\frac{b_1(t)(yh_3(t) + h_1(t)) + b_2(t)}{h_3(t)} + \frac{h_1'(t) + yh_3'(t)}{h_3(t)}\Big)\frac{\partial v}{\partial y}(y,t) \\ &+c(yh_3(t) + h_1(t), t)v(y,t) + f(yh_3(t) + h_1(t), t), \quad (y,t) \in Q_T,\end{aligned} \tag{8}$$

in the fixed domain $Q_T := \{(x,t)|\ 0 < y < 1, 0 < t < T\} = (0,1) \times (0,T)$,

$$v(y,0) = \varphi(yh_3(0) + h_1(0)), \quad y \in [0,1], \tag{9}$$

$$v(0,t)=\mu_1(t),\quad v(1,t)=\mu_2(t),\quad t\in[0,T], \tag{10}$$

$$h_1^{'}(t)-\frac{v_y(0,t)}{h_3(t)}=\mu_3(t),\quad t\in[0,T], \tag{11}$$

$$h_3^{'}(t)+\frac{v_y(0,t)+v_y(1,t)}{h_3(t)}+\mu_3(t)=\mu_4(t),\quad t\in[0,T], \tag{12}$$

$$h_3(t)\int_0^1 v(y,t)dy=\mu_5(t),\quad t\in[0,T], \tag{13}$$

$$h_3^2(t)\int_0^1 yv(y,t)dy+h_1(t)\mu_5(t)=\mu_6(t),\quad t\in[0,T]. \tag{14}$$

Definition 1. As a solution to the inverse problem (8)–(14), we consider the quintet $(h_1(t),h_3(t),b_1(t),b_2(t),v(y,t))\in(C^1[0,T])^2\times(C[0,T])^2\times C^{2,1}(\overline{Q_T})$, $h_3(t)>0$ for $t\in[0,T]$, that satisfies equations (8)–(14).

The local existence and uniqueness of the solution of problem (8)–(14) were established in [18] and read as follows.

Theorem 1. (Local existence of solution)
Assume that the following conditions hold:

$(A1)$ $a\in C^{1,0}(\mathbb{R}\times[0,T])$, $c,f\in H^{\alpha,0}(\mathbb{R}\times[0,T])$ *for some* $\alpha\in(0,1),\varphi\in C^2[h_{01},h_{02}]$, $\mu_i\in C^1[0,T], i=1,2,5,6$, $\mu_j\in C[0,T]$, $j=3,4$;

$(A2)$ $0<a_0\le a(x,t)\le a_1$, $c(x,t)\le 0$ *and* $f(x,t)\ge 0$ *for* $(x,t)\in\mathbb{R}\times[0,T]$, $\varphi(x)\ge\varphi_0>0$ *for* $x\in[h_{01},\infty)$, $\varphi'(x)>0$ *for* $x\in[h_{01},h_{02}]$, $\varphi'(x)-\varphi'(h_{02}+h_{01}-x)>0$ *and* $(h_{02}-x)\varphi'(h_{02}+h_{01}-x)-(x-h_{01})\varphi'(x)>0$ *for* $x\in\left[h_{01},\frac{h_{01}+h_{02}}{2}\right)$, $\mu_i(t)>0, i=1,2,5$, *for* $t\in[0,T]$.

$(A3)$ *Compatibility conditions of the zero and first orders.*
Then, it is possible to indicate a time $T_0\in(0,T]$, *determined by the input data, such that there exists a (local) solution to problem (8)–(14) for* $(y,t)\in Q_{T_0}$.

It is possible to determine the initial values $b_1(0)$ and $b_2(0)$, as follows. Differentiating (6) and (7) with respect to t we obtain

$$\int_{h_1(t)}^{h_2(t)}u_t(x,t)dx=\mu_5'(t)+\mu_2(t)u_x(h_2(t),t)+\mu_1(t)u_x(h_1(t),t)+\mu_1(t)\mu_3(t)-\mu_2(t)\mu_4(t), \tag{15}$$

$$\int_{h_1(t)}^{h_2(t)}xu_t(x,t)dx=\mu_6'(t)+\mu_2(t)u_x(h_2(t),t)h_2(t)+\mu_1(t)u_x(h_1(t),t)h_1(t)+\mu_1(t)\mu_3(t)h_1(t)-\mu_2(t)\mu_4(t)h_2(t). \tag{16}$$

Also, integrating (1) with respect to x we obtain

$$\int_{h_1(t)}^{h_2(t)} u_t(x,t)dx = \int_{h_1(t)}^{h_2(t)} \Big(a(x,t)u_{xx}(x,t) + c(x,t)u(x,t) + f(x,t)\Big)dx + b_1(t)\int_{h_1(t)}^{h_2(t)} xu_x(x,t)dx + b_2(t)\int_{h_1(t)}^{h_2(t)} u_x(x,t)dx, \tag{17}$$

$$\int_{h_1(t)}^{h_2(t)} xu_t(x,t)dx = \int_{h_1(t)}^{h_2(t)} x\Big(a(x,t)u_{xx}(x,t) + c(x,t)u(x,t) + f(x,t)\Big)dx + b_1(t)\int_{h_1(t)}^{h_2(t)} x^2u_x(x,t)dx + b_2(t)\int_{h_1(t)}^{h_2(t)} xu_x(x,t)dx. \tag{18}$$

Applying these equations at $t = 0$ and taking into account the compatibility conditions of the zero and first orders we obtain

$$\begin{cases} b_1(0)\int_{h_{01}}^{h_{02}} x\varphi'(x)dx + b_2(0)\int_{h_{01}}^{h_{02}} \varphi'(x)dx = \mu_5'(0) + \mu_2(0)\varphi'(h_{02}) + \mu_1(0)\varphi'(h_{01}) \\ +\mu_1(0)\mu_3(0) - \mu_2(0)\mu_4(0) - \int_{h_{01}}^{h_{02}} \Big(a(x,0)\varphi''(x) + c(x,0)\varphi(x) + f(x,0)\Big)dx =: R_1, \\ b_1(0)\int_{h_{01}}^{h_{02}} x^2\varphi'(x)dx + b_2(0)\int_{h_{01}}^{h_{02}} x\varphi'(x)dx = \mu_6'(0) + \mu_2(0)\varphi'(h_{02})h_{02} + \mu_1(0)\varphi'(h_{01})h_{01} \\ +\mu_1(0)\mu_3(0)h_{01} - \mu_2(0)\mu_4(0)h_{02} - \int_{h_{01}}^{h_{02}} x\Big(a(x,0)\varphi''(x) + c(x,0)\varphi(x) + f(x,0)\Big)dx =: R_2. \end{cases}$$

This system has the unique solution

$$\begin{cases} b_1(0) = \frac{R_1\int_{h_{01}}^{h_{02}} x\varphi'(x)dx - R_2\int_{h_{01}}^{h_{02}} \varphi'(x)dx}{\Delta}, \\ b_2(0) = \frac{R_2\int_{h_{01}}^{h_{02}} x\varphi'(x)dx - R_1\int_{h_{01}}^{h_{02}} x^2\varphi'(x)dx}{\Delta}, \end{cases} \tag{19}$$

provided that

$$\Delta = \left(\int_{h_{01}}^{h_{02}} x\varphi'(x)dx\right)^2 - \left(\int_{h_{01}}^{h_{02}} \varphi'(x)dx\right)\left(\int_{h_{01}}^{h_{02}} x^2\varphi'(x)dx\right) \neq 0. \tag{20}$$

Since $\varphi'(x) > 0$ applying Cauchy-Schwarz inequality to the functions $x\sqrt{\varphi'(x)}$ and $\sqrt{\varphi'(x)}$ it follows that $\Delta < 0$, hence the above solution for $b_1(0)$ and $b_2(0)$ always exists.

Theorem 2. (Local uniqueness of the solution)
Assume that the following conditions are satisfied:

$$a \in C^{2,0}(\mathbb{R}\times[0,T]),\ \varphi \in C^1[h_{01},h_{02}],\ c,f \in C^{1,0}(\mathbb{R}\times[0,T]),$$
$$a(x,t) > 0\ for\ (x,t) \in \mathbb{R}\times[0,T], \varphi(x) \geq \varphi_0 > 0\ for\ x \in [h_{01},\infty),$$
$$\varphi'(x) - \varphi'(h_{02}+h_{01}-x) > 0\ and\ (h_{02}-x)\varphi'(h_{02}+h_{01}-x) - (x-h_{01})\varphi'(x) > 0$$
$$for\ x \in \Big[h_{01}, \frac{h_{01}+h_{02}}{2}\Big),$$
$$\mu_i(t) > 0,\ i = 1,2,5,\ for\ t \in [0,T].$$

Then, it is possible to indicate a time $T_1 \in (0,T]$, determined by the input data, such that problem (8)–(14) cannot have two different solutions for $(y,t) \in Q_{T_1}$.

2.1 Related inverse problem statement

A related inverse problem has been considered in [20], where the Stefan conditions (4) and (5) (or (11) and (12)), were replaced by the second and third-order heat moment measurement

$$\int_{h_1(t)}^{h_2(t)} x^{i-5}u(x,t)dx = \mu_i(t), \quad i = 7,8, \quad t \in [0,T], \tag{21}$$

or, in terms of change of variable $y = \frac{x-h_1(t)}{h_2(t)-h_1(t)}$,

$$h_3^3(t)\int_0^1 y^2 v(y,t)dy + 2h_1(t)\mu_6(t) - h_1^2(t)\mu_5(t) = \mu_7(t), \quad t \in [0,T], \tag{22}$$

$$h_3^4(t)\int_0^1 y^3 v(y,t)dy + 3h_1(t)\mu_7(t) - 3h_1^2(t)\mu_6(t) + h_1^3(t)\mu_5(t) = \mu_8(t), \quad t \in [0,T]. \tag{23}$$

Definition 1 still applies for the solution of the inverse problem (8)–(10), (13), (14), (22) and (23), which is concerned with the invertibility of the map $(\mu_5, \mu_6, \mu_7, \mu_8) \mapsto (h_1, h_2, b_1, b_2)$.

The local existence and uniqueness to this problem were established in [20] and read as follows.

Theorem 3. (Local existence of solution)
Assume that conditions (A2) and (A3) of Theorem 1 are satisfied and that
(A4) a, c, $f \in C^{1,0}(\mathbb{R}\times[0,T])$, $\varphi \in C^2[h_{01}, h_{02}]$, $\mu_i \in C^1[0,T], i = 1,2,5,6,7,8$.
Then, it is possible to indicate a time $T_2 \in (0,T]$, *determined by the input data, such that there exists a (local) solution to problem (8)–(10), (13), (14), (22) and (23) for* $(y,t) \in Q_{T_2}$.

As in the previous problem, we can deduce the following system of equations for the unknowns $b_1(0)$, $b_2(0)$, $h_1'(0)$ and $h_2'(0)$:

$$\begin{aligned} b_1(0)\int_{h_{01}}^{h_{02}} x^{k+1}\varphi'(x)dx + b_2(0)\int_{h_{01}}^{h_{02}} x^k\varphi'(x)dx + \mu_2(0)h_{02}^k h_2'(0) - \mu_1(0)h_{01}^k h_1'(0) \\ = \mu_{k+5}'(0) - \int_{h_{01}}^{h_{02}} x^k\Big(a(x,0)\varphi''(x) + c(x,0)\varphi(x) + f(x,0)\Big)dx =: P_k, \\ k = 0,1,2,3. \end{aligned} \tag{24}$$

Theorem 4. (Local uniqueness of the solution)
Assume that the conditions of Theorem 2 are satisfied. Then, it is possible to indicate a time $T_3 \in (0,T]$, *determined by the input data, such that problem (8)–(10), (13), (14), (22) and (23) cannot have two different solutions for* $(y,t) \in Q_{T_3}$.

3 Numerical solution of direct problem

Consider the direct initial boundary value problem given by equations (8)–(10), where $h_1(t)$, $h_2(t)$, $b_1(t)$, $b_2(t)$, $a(x,t)$, $c(x,t)$, $f(x,t)$, $\varphi(x)$, $\mu_1(t)$ and $\mu_2(t)$ are known and the solution $v(y,t)$ is to be determined together with the quantities of interest $\mu_i(t)$, $i=\overline{3,8}$. To achieve this, we use the FDM with the Crank-Nicolson scheme, [21], based on subdividing the solution $Q_T=(0,1)\times(0,T)$ into M and N subintervals of equal lengths Δy and Δt, where $\Delta y=1/M$ and $\Delta t=T/N$, respectively. At the node (i,j) we denote $v(y_i,t_j)=v_{i,j}$, where $y_i=i\Delta y$, $t_j=j\Delta t$, $a(y_i,t_j)=a_{i,j}$, $c(y_i,t_j)=c_{i,j}$, $h_1(t_j)=h_{1_j}$, $h_3(t_j)=h_2(t_j)-h_1(t_j)=h_{3_j}$, $b_1(t_j)=b_{1_j}$, $b_2(t_j)=b_{2_j}$, and $f(y_i,t_j)=f_{i,j}$ for $i=\overline{0,M}$ and $j=\overline{0,N}$. Based on the FDM, equation (8) can be approximated as:

$$\begin{aligned}&-A_{i,j+1}v_{i-1,j+1}+(1+B_{i,j+1})v_{i,j+1}-C_{i,j+1}v_{i+1,j+1}\\&\quad=A_{i,j}v_{i-1,j}+(1-B_{i,j})v_{i,j}+C_{i,j}v_{i+1,j}+\frac{\Delta t}{2}(f_{i,j}+f_{i,j+1}),\end{aligned}\tag{25}$$

for $i=\overline{1,(M-1)}$, $j=\overline{0,N}$, where

$$\begin{aligned}A_{i,j}=\frac{(\Delta t)\zeta_{i,j}}{2(\Delta y)^2}-\frac{(\Delta t)\eta_{i,j}}{4(\Delta y)},\quad B_{i,j}=\frac{(\Delta t)\zeta_{i,j}}{(\Delta y)^2}-\frac{(\Delta t)c_{i,j}}{2},\quad C_{i,j}=\frac{(\Delta t)\zeta_{i,j}}{2(\Delta y)^2}+\frac{(\Delta t)\eta_{i,j}}{4(\Delta y)},\\ \zeta_{i,j}=\frac{a_{i,j}}{h_{3_j}^2},\quad \eta_{i,j}=\frac{b_{1_j}(y_ih_{3_j}+h_{1_j})+b_{2_j}+h'_{1_j}+y_ih'_{3_j}}{h_{3_j}}.\end{aligned}\tag{26}$$

The initial and boundary conditions in equations (9) and (10) are discretized as

$$v_{i,0}=\varphi(y_ih_{03}+h_{01}),\quad i=\overline{0,M},\tag{27}$$

where $h_{03}=h_3(0)$,

$$v_{0,j}=\mu_1(t_j),\quad v_{M,j}=\mu_2(t_j),\quad j=\overline{0,N}.\tag{28}$$

At each time step t_{j+1}, for $j=\overline{0,(N-1)}$, using the Dirichlet boundary conditions (28), the difference equation (25) can be reformulated as a $(M-1)\times(M-1)$ system of linear equations of the form,

$$G\mathbf{v_{j+1}}=H\mathbf{v_j}+\mathbf{r},\tag{29}$$

where

$$\mathbf{v_{j+1}}=(v_{1,j+1},v_{2,j+1},...,v_{M-2,j+1},v_{M-1,j+1})^{\mathrm{T}},$$

$$G=\begin{pmatrix}1+B_{1,j+1}&-C_{1,j+1}&0&...&0&0&0\\-A_{2,j+1}&1+B_{2,j+1}&-C_{2,j+1}&...&0&0&0\\\vdots&\vdots&\vdots&\ddots&\vdots&\vdots&\vdots\\0&0&0&...&-A_{M-2,j+1}&1+B_{M-2,j+1}&-C_{M-2,j+1}\\0&0&0&...&0&-A_{M-1,j+1}&1+B_{M-1,j+1}\end{pmatrix},$$

$$H=\begin{pmatrix} 1-B_{1,j} & C_{1,j} & 0 & ... & 0 & 0 & 0 \\ A_{2,j} & 1-B_{2,j} & C_{2,j} & ... & 0 & 0 & 0 \\ \vdots & \vdots & \vdots & \ddots & \vdots & \vdots & \vdots \\ 0 & 0 & 0 & ... & A_{M-2,j} & 1-B_{M-2,j} & C_{M-2,j} \\ 0 & 0 & 0 & ... & 0 & A_{M-1,j} & 1-B_{M-1,j} \end{pmatrix},$$

$$\mathbf{r}=\begin{pmatrix} A_{1,j}\mu_1(t_j)+A_{1,j+1}\mu_1(t_{j+1})+\frac{\Delta t}{2}(f_{1,j}+f_{1,j+1}) \\ \frac{\Delta t}{2}(f_{2,j}+f_{2,j+1}) \\ \vdots \\ \frac{\Delta t}{2}(f_{M-2,j}+f_{M-2,j+1}) \\ C_{M-1,j}\mu_2(t_j)+C_{M-1,j+1}\mu_2(t_{j+1})+\frac{\Delta t}{2}(f_{M-1,j}+f_{M-1,j+1}) \end{pmatrix}.$$

The expressions (11)–(14), (22) and (23) can be approximated using the following finite difference approximation formulae and trapezoidal rule for integrals:

$$\mu_3(t_j)=\frac{h_{1_j}-h_{1_{j-1}}}{\Delta t}-\frac{4v_{1,j}-v_{2,j}-3v_{0,j}}{2(\Delta y)h_{3_j}},\quad j=\overline{1,N}, \tag{30}$$

$$\mu_4(t_j)=\frac{h_{3_j}-h_{3_{j-1}}}{\Delta t}+\Big(\frac{4v_{1,j}-v_{2,j}-3v_{0,j}}{2(\Delta y)h_{3_j}}-\frac{4v_{M-1,j}-v_{M-2,j}-3v_{M,j}}{2(\Delta y)h_{3_j}}\Big) +\mu_3(t_j),\quad j=\overline{1,N}, \tag{31}$$

$$\mu_{k+4}(t_j)=\frac{h_{3_j}^k}{2N}\Big(y_0^{k-1}v_{0,j}+y_M^{k-1}v_{M,j}+2\sum_{i=1}^{M-1}y_i^{k-1}v_{i,j}\Big),\quad j=\overline{1,N},\quad k=\overline{1,4}. \tag{32}$$

4 Numerical solution of inverse problem

For the inverse problems described in Section 2, our aim is to obtain simultaneously stable reconstructions of the two unknown coefficients $b_1(t)$ and $b_2(t)$, together with the moving boundaries $h_1(t)$ and $h_3(t)$, and the transformed temperature $v(y,t)$, satisfying the equations (8)–(14) or, (8)–(10), (13), (14), (22) and (23), by minimizing the nonlinear Tikhonov regularization function

$$F(\mathbf{h_1},\mathbf{h_3},\mathbf{b_1},\mathbf{b_2})=\sum_{j=1}^{N}\Big[h'_{1_j}-\frac{v_y(0,t_j)}{h_{3_j}}-\mu_3(t_j)\Big]^2+\sum_{j=1}^{N}\Big[h'_{3_j}+\frac{v_y(0,t_j)+v_y(1,t_j)}{h_{3_j}} +\mu_3(t_j)-\mu_4(t_j)\Big]^2+\sum_{j=1}^{N}\Big[h_{3_j}\int_0^1 v(y,t_j)dy-\mu_5(t_j)\Big]^2+\sum_{j=1}^{N}\Big[h_{3_j}^2\int_0^1 yv(y,t_j)dy +h_1(t_j)\mu_5(t_j)-\mu_6(t_j)\Big]^2+\beta_1\sum_{j=1}^{N}h_{1_j}^2+\beta_2\sum_{j=1}^{N}h_{3_j}^2+\beta_3\sum_{j=1}^{N}b_{1_j}^2+\beta_4\sum_{j=1}^{N}b_{2_j}^2, \tag{33}$$

or,

$$F_1(\mathbf{h_1},\mathbf{h_3},\mathbf{b_1},\mathbf{b_2}) = \sum_{j=1}^{N}\Big[h_{3_j}\int_0^1 v(y,t_j)dy - \mu_5(t_j)\Big]^2 + \sum_{j=1}^{N}\Big[h_{3_j}^2\int_0^1 yv(y,t_j)dy + h_1(t_j)\mu_5(t_j) - \mu_6(t_j)\Big]^2 + \sum_{j=1}^{N}\Big[h_{3_j}^3\int_0^1 y^2v(y,t_j)dy + 2h_1(t_j)\mu_6(t_j) - h_1^2(t_j)\mu_5(t_j) - \mu_7(t_j)\Big]^2 + \sum_{j=1}^{N}\Big[h_{3_j}^4\int_0^1 y^3v(y,t_j)dy + 3h_1(t_j)\mu_7(t_j) - 3h_1^2(t_j)\mu_6(t_j) + h_1^3(t_j)\mu_5(t_j) - \mu_8(t_j)\Big]^2 + \beta_1\sum_{j=1}^{N}h_{1_j}^2 + \beta_2\sum_{j=1}^{N}h_{3_j}^2 + \beta_3\sum_{j=1}^{N}b_{1_j}^2 + \beta_4\sum_{j=1}^{N}b_{2_j}^2, \quad (34)$$

respectively, where v solves (8)–(10) for given $(\mathbf{h_1},\mathbf{h_3},\mathbf{b_1},\mathbf{b_2})$, and $\beta_i \geq 0$ for $i = \overline{1,4}$ are regularization parameters to be prescribed. The minimization of F, or F_1, is performed using the MATLAB toolbox routine *lsqnonlin*, which does not require the user to supply the gradient of the objective function, [14]. This routine attempts to find the minimum of a sum of squares by starting from an arbitrary initial guesses, subject to the physical constraint $h_3(t) > 0$. Thus, we take the lower and upper simple bounds for $h_3(t)$ to be 10^{-8} and 10^3, respectively, and the lower and upper bounds for the quantities $h_1(t)$, $b_1(t)$ and $b_2(t)$ to be -10^3 and 10^3, respectively. Furthermore, within *lsqnonlin*, we use the Trust Region Reflective (TRR) algorithm [5], which is based on the interior-reflective Newton method. We also take the parameters of the routine as follows:

- Maximum number of iterations, (MaxIter)= 10×(number of variables).
- Maximum number of objective function evaluations, (MaxFunEvals) = $10^5\times$ (number of variables).
- Termination tolerance on the function value, (TolFun) = 10^{-20}.
- Solution tolerance, (XTol) = 10^{-20}.

In the expressions (26) and (33), we approximate the derivatives of $h_1(t)$ and $h_3(t)$ as

$$h'_{1_j} := h_1'(t_j) \approx \frac{h_1(t_j) - h_1(t_{j-1})}{\Delta t} = \frac{h_{1_j} - h_{1_{j-1}}}{\Delta t}, \quad j = \overline{1,N}, \quad (35)$$

$$h'_{3_j} := h_3'(t_j) \approx \frac{h_3(t_j) - h_3(t_{j-1})}{\Delta t} = \frac{h_{3_j} - h_{3_{j-1}}}{\Delta t}, \quad j = \overline{1,N}. \quad (36)$$

The measured data are (4)–(7) and (21). In order to model the errors in this data, we replace $\mu_{k+2}(t_j)$, $k = \overline{1,6}$, in equations (11)–(14) or, (22) and (23) by $\mu_{k+2}^{\epsilon k}(t_j)$, as

$$\mu_{k+2}^{\epsilon k}(t_j) = \mu_{k+2}(t_j) + \epsilon k_j, \quad k = \overline{1,6}, \quad j = \overline{1,N}, \quad (37)$$

where ϵk_j are random variables generated from a Gaussian normal distribution with mean zero and standard deviation σ_k given by

$$\sigma_k = p \times \max_{t\in[0,T]} |\mu_{k+2}(t)|, \quad k = \overline{1,6}, \tag{38}$$

where p represents the percentage of noise.

5 Numerical results and discussion

In this section, we present a couple of benchmark numerical test examples to illustrate the accuracy and stability of the numerical methods based on the FDM with Crank-Nicolson scheme combined with the minimization of the objective function F, or F_1, as described in Section 4. Furthermore, we add noise to the input measurement data (11)–(14), (22) and (23) to simulate the real situation of measurement noisy data, by using equations (37) and (38). To quantify the accuracy of the approximate solution, we employ the root mean squares error (rmse) defined by

$$\text{rmse}(h_1) = \left[\frac{T}{N}\sum_{j=1}^{N}\left(h_1^{Numerical}(t_j) - h_1^{Exact}(t_j)\right)^2\right]^{1/2}, \tag{39}$$

and similar expressions exist for $h_3(t)$, $b_1(t)$ and $b_2(t)$. For simplicity, we take $T = 1$ in all examples.

5.1 Example 1 (for inverse problem I)

We consider the first inverse problem given by (1)–(7) with unknown coefficients $h_1(t)$, $h_2(t)$, $b_1(t)$ and $b_2(t)$, and solve this with the following input data:

$$\begin{gathered}
a(x,t) = \frac{1}{100}(1+t) + x, \quad c(x,t) = -1 - x - t, \quad \varphi(x) = \pi + \tan^{-1}(x), \\
\mu_1(t) = (1+t)\Big(\pi + \tan^{-1}\Big(\frac{5+t}{10}\Big)\Big), \quad \mu_2(t) = (1+t)\Big(\pi + \tan^{-1}\Big(\frac{15+2t}{10}\Big)\Big), \\
f(x,t) = \pi + \frac{(1+t)x(1+t+100x)}{50\,(1+x^2)^2} - \frac{t(1+t)(1+x)}{1+x^2} + \tan^{-1}(x) \\
+(1+t)(1+t+x)(\pi + \tan^{-1}(x)),
\end{gathered} \tag{40}$$

$$\mu_3(t) = \frac{1}{10} - \frac{1+t}{1+\left(\frac{1}{2}+\frac{t}{10}\right)^2}, \quad \mu_4(t) = \frac{1}{5} + \frac{1+t}{1+\left(\frac{3}{2}+\frac{t}{5}\right)^2}, \quad t \in [0,T], \tag{41}$$

$$\begin{aligned}
\mu_5(t) = \frac{1}{10}(1+t)\Big[10\pi + \pi t + (15+2t)\tan^{-1}\Big(\frac{15+2t}{10}\Big) - (5+t)\tan^{-1}\Big(\frac{5+t}{10}\Big) \\
+5\ln\Big(\frac{125+t(10+t)}{325+4t(15+t)}\Big)\Big], \quad t \in [0,T],
\end{aligned} \tag{42}$$

$$\mu_6(t) = \frac{1}{200}(1+t)\Big[(10+t)\Big(-10+\pi(20+3t)\Big) + \Big(325+4t(15+t)\Big)\tan^{-1}\Big(\frac{15+2t}{10}\Big) - \Big(125+t(10+t)\Big)\tan^{-1}\Big(\frac{5+t}{10}\Big)\Big], \quad t\in[0,T]. \tag{43}$$

Remark that conditions of Theorems 1 and 2 are satisfied and therefore, the local existence and uniqueness of the solution are guaranteed. In fact, one can easily check that the analytical solution of the transformed inverse problem (8)–(14) is given by

$$v(y,t) = u(yh_3(t)+h_1(t),t) = (1+t)\Big(\pi+\tan^{-1}\Big(\frac{1}{10}(5+t+10y+ty)\Big)\Big), \tag{44}$$

$$h_1(t) = \frac{1}{2}+\frac{t}{10}, \quad h_2(t) = \frac{3}{2}+\frac{t}{5}, \quad b_1(t) = t, \quad b_2(t) = t. \tag{45}$$

Also,

$$u(x,t) = (1+t)\Big(\pi+\tan^{-1}(x)\Big). \tag{46}$$

In the direct problem given by (8)–(10) and (45), the numerical results for the interior transformed temperature $v(y,t)$ have been obtained in excellent agreement with the analytical solution (44) and therefore, they are not presented. Apart from the interior transformed temperature $v(y,t)$, other outputs of interest are the overdetermination data (4)–(7), which analytically are given by (41)–(43). Table 1 shows that the analytical and numerical solutions for these quantities obtained with various mesh sizes $M = N \in \{10, 20, 40\}$ are in very good agreement.

Table 1: The analytical and numerical solutions for $\mu_k(t)$, $k = \overline{3,8}$, with $M = N \in \{10, 20, 40\}$, for the direct problem.

t	0.1	0.2	0.3	...	0.8	0.9	1	
$\mu_3(t)$	-0.7732	-0.8444	-0.9147	...	-1.2451	-1.3072	-1.3679	$M = N = 10$
	-0.7731	-0.8447	-0.9150	...	-1.2466	-1.3090	-1.3701	$M = N = 20$
	-0.7730	-0.8446	-0.9149	...	-1.2469	-1.3093	-1.3705	$M = N = 40$
	-0.7729	-0.8446	-0.9149	...	-1.2469	-1.3094	-1.3706	exact
$\mu_4(t)$	0.5320	0.5551	0.5779	...	0.6778	0.6955	0.7124	$M = N = 10$
	0.5322	0.5559	0.5786	...	0.6791	0.6969	0.7140	$M = N = 20$
	0.5323	0.5559	0.5786	...	0.6793	0.6971	0.7141	$M = N = 40$
	0.5323	0.5559	0.5786	...	0.6793	0.6971	0.7141	exact
$\mu_5(t)$	4.3474	4.7984	5.2587	...	7.7009	8.2176	8.7436	$M = N = 10$
	4.3478	4.7988	5.2592	...	7.7018	8.2185	8.7446	$M = N = 20$
	4.3479	4.7990	5.2594	...	7.7020	8.2187	8.7448	$M = N = 40$
	4.3479	4.7990	5.2594	...	7.7021	8.2188	8.7449	exact
$\mu_6(t)$	4.4615	4.9966	5.5550	...	8.7139	9.4220	10.1566	$M = N = 10$
	4.4610	4.9960	5.5544	...	8.7130	9.4211	10.1556	$M = N = 20$
	4.4608	4.9958	5.5542	...	8.7128	9.4208	10.1553	$M = N = 40$
	4.4608	4.9958	5.5541	...	8.7127	9.4208	10.1552	exact
$\mu_7(t)$	4.9522	5.6234	6.3379	...	10.6167	11.6254	12.6891	$M = N = 10$
	4.9461	5.6166	6.3303	...	10.6044	11.6121	12.6746	$M = N = 20$
	4.9446	5.6149	6.3284	...	10.6014	11.6087	12.6710	$M = N = 40$
	4.9441	5.6143	6.3277	...	10.6004	11.6076	12.6698	exact
$\mu_8(t)$	5.8339	6.7142	7.6683	...	13.6917	15.1780	16.7692	$M = N = 10$
	5.8248	6.7039	7.6567	...	13.6721	15.1565	16.7457	$M = N = 20$
	5.8226	6.7013	7.6538	...	13.6672	15.1512	16.7399	$M = N = 40$
	5.8218	6.7005	7.6528	...	13.6656	15.1494	16.7379	exact

In the inverse problem (8)–(14), we take the initial guesses for the vectors $\mathbf{h_1}$, $\mathbf{h_3}$, $\mathbf{b_1}$ and $\mathbf{b_2}$ as follows:

$$h^0_{1_j} = h_{01} = 0.5,\ h^0_{3_j} = h_{02} - h_{01} = 1,\ b^0_{1_j} = b_1(0) = 0,\ b^0_{2_j} = b_2(0) = 0,\ j = \overline{1, N}. \quad (47)$$

Note that the values of $b_1(0)$ and $b_2(0)$ are available from (19).

We start the investigation for reconstructing the time-dependent unknowns coefficients $h_1(t)$, $h_3(t)$, $b_1(t)$ and $b_2(t)$, when there is no noise in the input data (11)–(14), i.e. $p = 0$ in (38). The objective function F, as a function of the number of iterations, is plotted (curve $-\square-$) in Figures 2 and 3, for no noise, without and with regularization, respectively. From these figures, it can be seen that a rapid monotonic decreasing convergence to a very low value of $O(10^{-24})$ is achieved in about 16 iterations in the case of no regularization, i.e. $\beta_i = 0$, $i = \overline{1, 4}$, and of $O(10^{-6})$ in the case of regularization with $\beta_1 = \beta_2 = 0$, $\beta_3 = \beta_4 = 10^{-7}$.

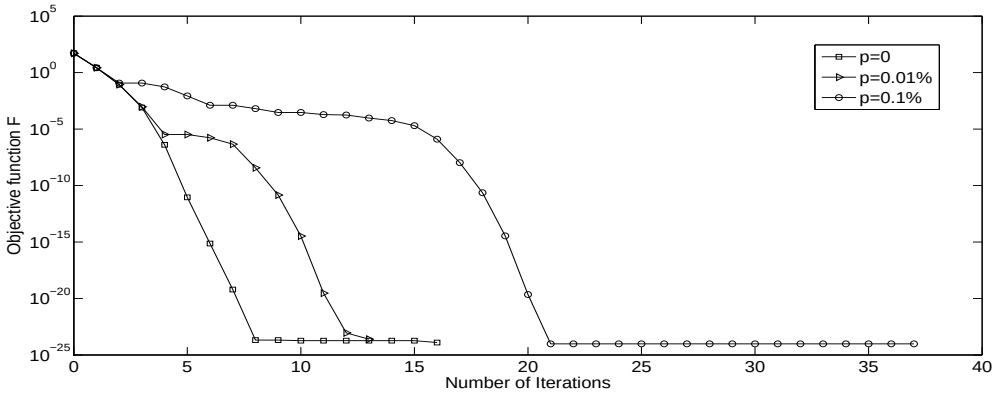

Figure 2: The objective function F, as a function of the number of iterations, for $p \in \{0, 0.01\%, 0.1\%\}$ noise, no regularization, for Example 1.

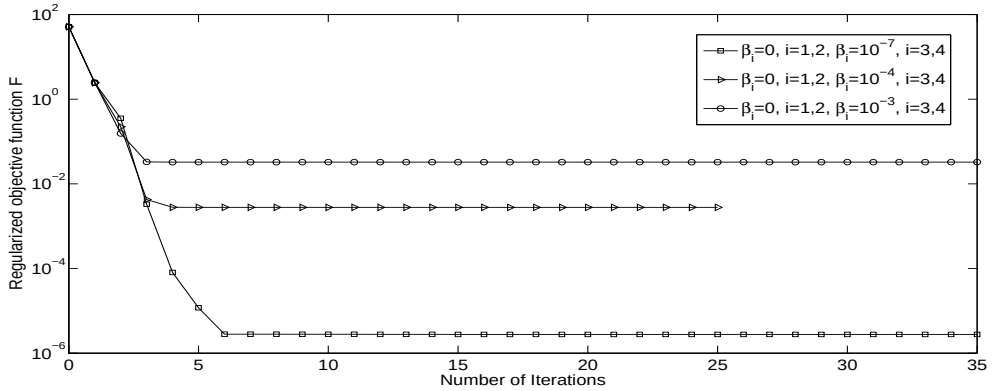

Figure 3: The regularized objective function F, as a function of the number of iterations, for noise $p = 0$ $(-\square-)$, $p = 0.01\%$ $(-\triangleright-)$ and $p = 0.1\%$ $(-\circ-)$, with regularization, for Example 1.

The analytical (44) and numerical solutions for the transformed temperature $v(y,t)$, with no noise, with and without regularizarion are shown in Figure 4.

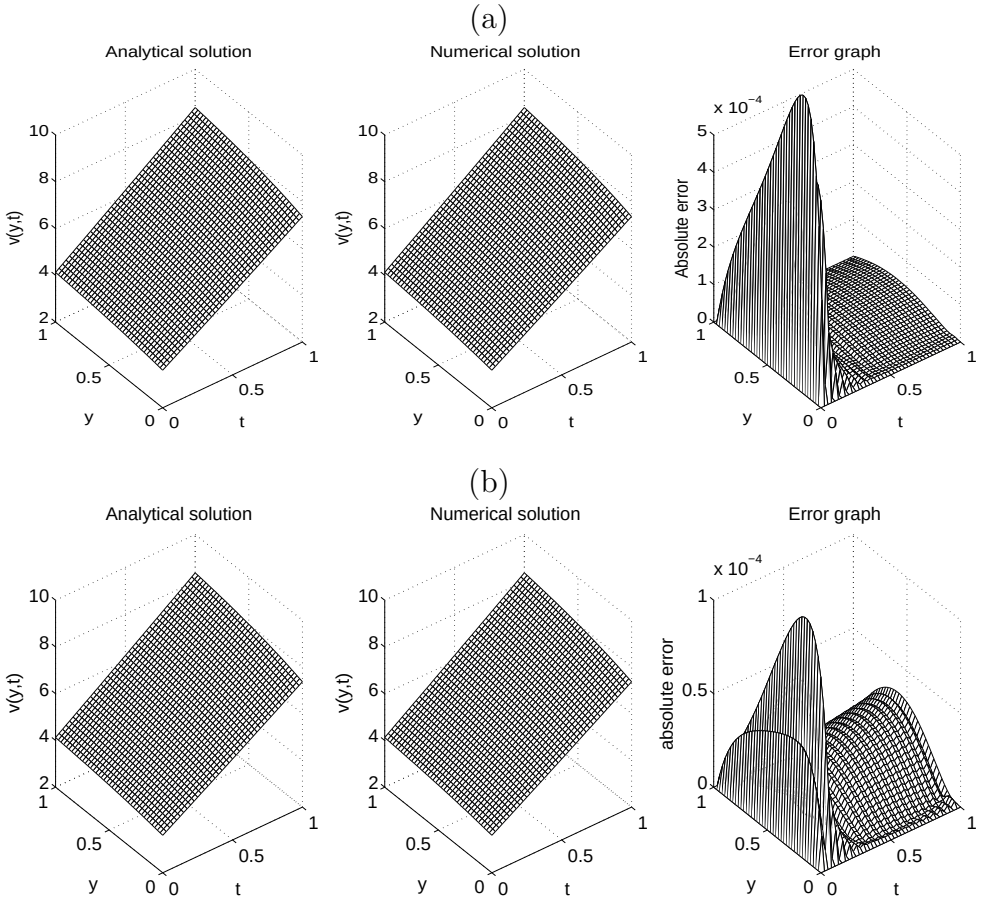

Figure 4: The analytical (44) and numerical solutions for the transformed temperature $v(y,t)$, for Example 1, no noise, with $\beta_1 = \beta_2 = 0$ and: (a) $\beta_3 = \beta_4 = 0$ and (b) $\beta_3 = \beta_4 = 10^{-7}$. The absolute error between them is also included.

From this figure, it can be noticed that the inverse problem is stable and accurate in the transformed temperature $v(y,t)$. The $rmse$ values for the unknowns coefficients $h_1(t)$, $h_3(t)$, $b_1(t)$ and $b_2(t)$ are presented in Figure 5 with and without regularization, versus the number of iterations. It can be seen that the $rmse$ values settle rapidly to stationary values after 5 to 6 iterations. It can also be observed that $rmse(h_1)$ and $rmse(h_3)$ values are much lower than the $rmse(b_1)$ and $rmse(b_2)$, pointing out that the free boundaries $h_1(t)$ and $h_3(t)$ are recovered more accurately than the coefficients $b_1(t)$ and $b_2(t)$.

The numerical results presented in Figure 6 show that although the retrieval of free boundaries $h_1(t)$ and $h_3(t)$, see Figures 6(a) and 6(b), are very accurate, some slight instability starts to manifest in the unregularization solutions for the coefficients $b_1(t)$ and $b_2(t)$, see Figures 6(c) and 6(d), respectively.

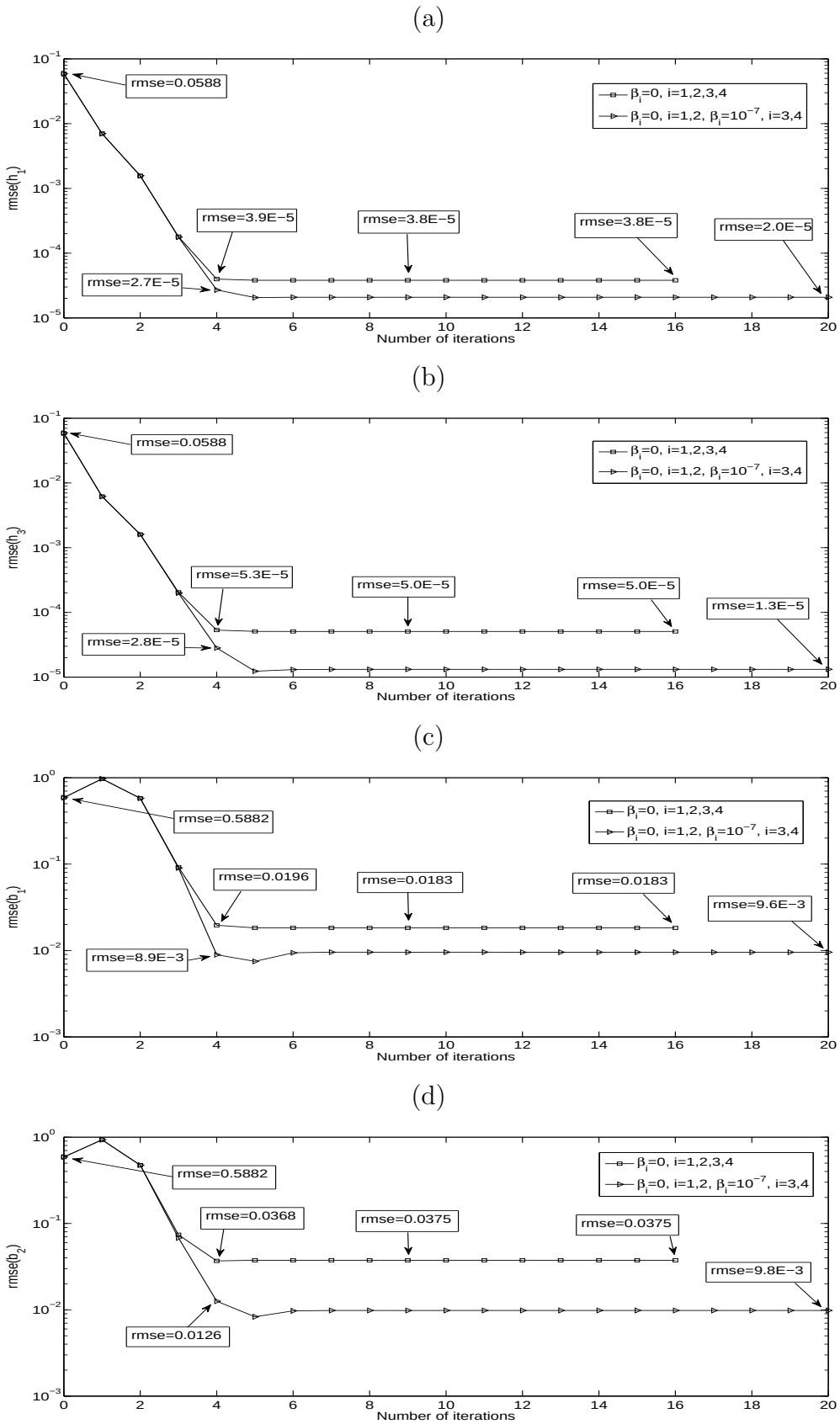

Figure 5: The *rmse* values: (a) $h_1(t)$, (b) $h_3(t)$, (c) $b_1(t)$ and (d) $b_2(t)$, as functions of the number of iterations, no noise, with and without regularization, for Example 1.

(a)

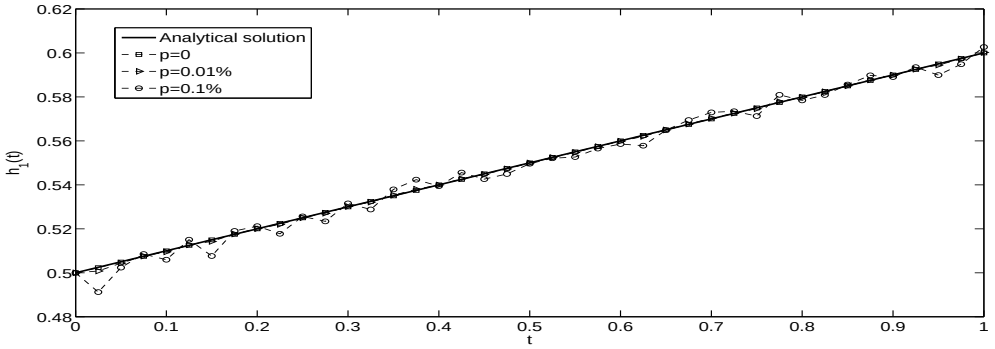

(b)

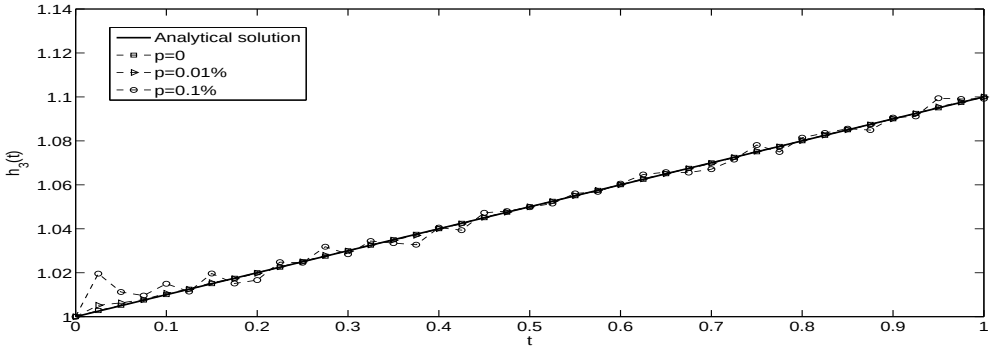

(c)

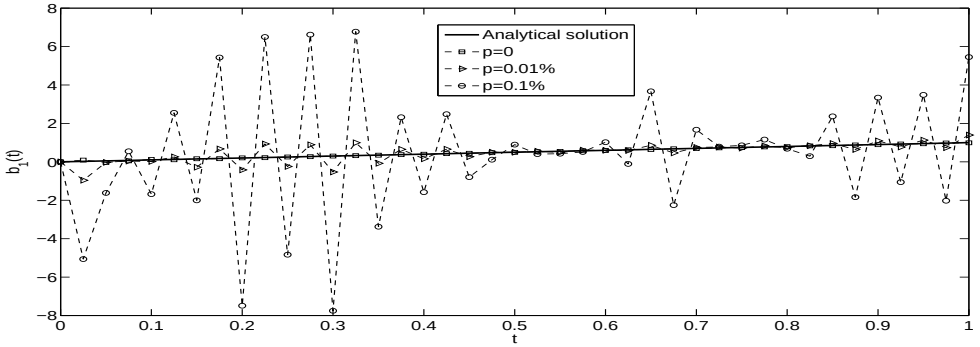

(d)

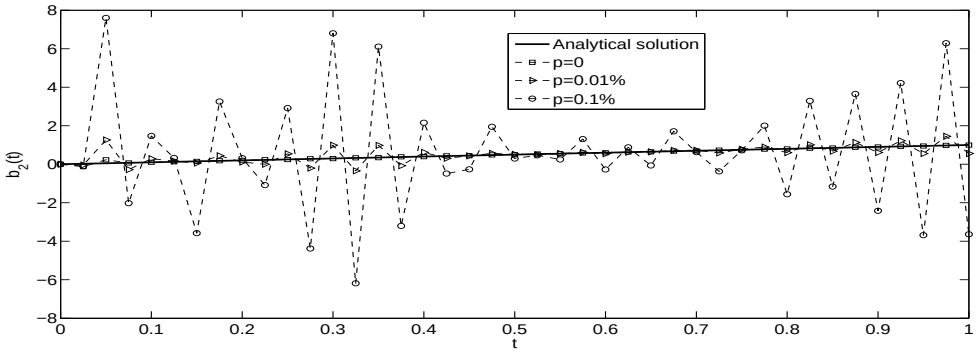

Figure 6: The analytical (45) and numerical solutions for: (a) $h_1(t)$, (b) $h_3(t)$, (c) $b_1(t)$ and (d) $b_2(t)$, for $p \in \{0, 0.01\%, 0.1\%\}$ noise, no regularization, for Example 1.

Thus, some slight regularization with, $\beta_1 = \beta_2 = 0$, $\beta_3 = \beta_4 = 10^{-7}$, is applied in order to obtain stable and accurate solutions for the coefficients $b_1(t)$ and $b_2(t)$, see Figures 8(c) and 8(d). As the numerical results for the free boundaries h_1 and h_3 have been found stable, in the remaining of the paper we take $\beta_1 = \beta_2 = 0$ and vary only the regularization parameter $\beta_3 = \beta_4 > 0$.

Next, we investigate the stability of the numerical solution with respect to various levels of $p \in \{0.01\%, 0.1\%\}$ noise in (38) included in the input data $\mu_3(t)$, $\mu_4(t)$, $\mu_5(t)$ and $\mu_6(t)$. From the previous discussion, we anticipate that regularization is required in order to obtain stable and accurate solutions because the inverse problem is ill-posed. The L-curve, [8], for the choice of the regularization parameter is shown in Figure 7, by plotting the solution norm $\sqrt{||\mathbf{h_1}||^2+||\mathbf{h_3}||^2+||\mathbf{b_1}||^2+||\mathbf{b_1}||^2}$, as a function of the residual norm given by square root of the sum of first four terms in the rigth-hand side of equation (33). Form this figure, it can be observed that regularization parameters near the "corner" of the L-curve are $\beta_3 = \beta_4 \in \{10^{-5}, 10^{-4}\}$ for $p = 0.01\%$ noise, and $\beta_3 = \beta_4 \in \{10^{-5}, 10^{-4}, 10^{-3}\}$ for $p = 0.1\%$.

The decreasing monotonic convergence of the objective function F, as a function of the number of iterations, without and with regularization are shown in Figures 2 and 3, respectively. In case of no regularization, Figure 2 shows that convergence is more rapidly achieved as the amount of noise p decreases. In order to stabilise the coefficients $b_1(t)$ and $b_2(t)$, we employ regularization with $\beta_3 = \beta_4 = 10^{-4}$ (suggested by the L-curve in Figure 7(a)), obtaining $rmse(b_1) = 0.0469$ and $rmse(b_2) = 0.0526$ for $p = 0.01\%$ noise, and with $\beta_3 = \beta_4 = 10^{-3}$ (suggested by the L-curve in Figure 7(b)), obtaining $rmse(b_1) = 0.0999$ and $rmse(b_2) = 0.1018$ for $p = 0.1\%$ noise. Numerical results are shown in Figure 8. For more, information about the $rmse$ values for various levels of noise and with and without regularization, see Table 2.

Table 2: The $rmse$ values for $p \in \{0, 0.01\%, 0.1\%\}$ noise, with and without regularization, for Example 1.

p	Regularization	$rmse(h_1)$	$rmse(h_3)$	$rmse(b_1)$	$rmse(b_2)$
0	$\beta_i = 0, i = \overline{1,4}$	3.8E-5	5.0E-5	0.0183	0.0375
	$\beta_3 = \beta_4 = 10^{-8}$	2.0E-5	1.3E-5	9.5E-3	9.9E-3
	$\beta_3 = \beta_4 = 10^{-7}$	**2.0E-5**	**1.3E-5**	**9.6E-3**	**9.8E-3**
	$\beta_3 = \beta_4 = 10^{-6}$	2.0E-5	1.1E-5	0.0107	0.0101
	$\beta_3 = \beta_4 = 10^{-5}$	2.8E-5	1.6E-5	0.0195	0.0164
0.01%	$\beta_i = 0, i = \overline{1,4}$	4.0E-4	5.2E-4	0.3523	0.3406
	$\beta_3 = \beta_4 = 10^{-8}$	3.6E-4	4.2E-4	2.1264	2.1329
	$\beta_3 = \beta_4 = 10^{-7}$	3.4E-4	3.8E-4	0.3124	0.3030
	$\beta_3 = \beta_4 = 10^{-6}$	3.0E-4	2.8E-4	0.2043	0.2311
	$\beta_3 = \beta_4 = 10^{-5}$	2.3E-4	1.6E-4	0.0799	0.1099
	$\beta_3 = \beta_4 = 10^{-4}$	**1.9E-4**	**1.3E-4**	**0.0469**	**0.0526**
	$\beta_3 = \beta_4 = 10^{-3}$	7.1E-4	5.0E-4	0.0931	0.0822
	$\beta_3 = \beta_4 = 10^{-2}$	3.5E-3	2.6E-3	0.1896	0.1610
	$\beta_3 = \beta_4 = 10^{-1}$	0.0183	0.0112	0.3260	0.2793
0.1%	$\beta_i = 0, i = \overline{1,4}$	3.4E-3	3.7E-3	3.3290	3.0690
	$\beta_3 = \beta_4 = 10^{-8}$	3.5E-3	4.2E-3	3.0069	3.0316
	$\beta_3 = \beta_4 = 10^{-7}$	3.5E-3	4.4E-3	2.8401	2.9265
	$\beta_3 = \beta_4 = 10^{-6}$	3.2E-3	3.5E-3	1.7770	2.2791
	$\beta_3 = \beta_4 = 10^{-5}$	2.4E-3	1.8E-3	0.8622	1.0312
	$\beta_3 = \beta_4 = 10^{-4}$	1.7E-3	1.2E-3	0.3243	0.3048
	$\beta_3 = \beta_4 = 10^{-3}$	**1.3E-3**	**9.5E-4**	**0.0999**	**0.1018**
	$\beta_3 = \beta_4 = 10^{-2}$	3.6E-3	2.8E-3	0.1799	0.1542
	$\beta_3 = \beta_4 = 10^{-1}$	0.0154	0.0115	0.3251	0.2791

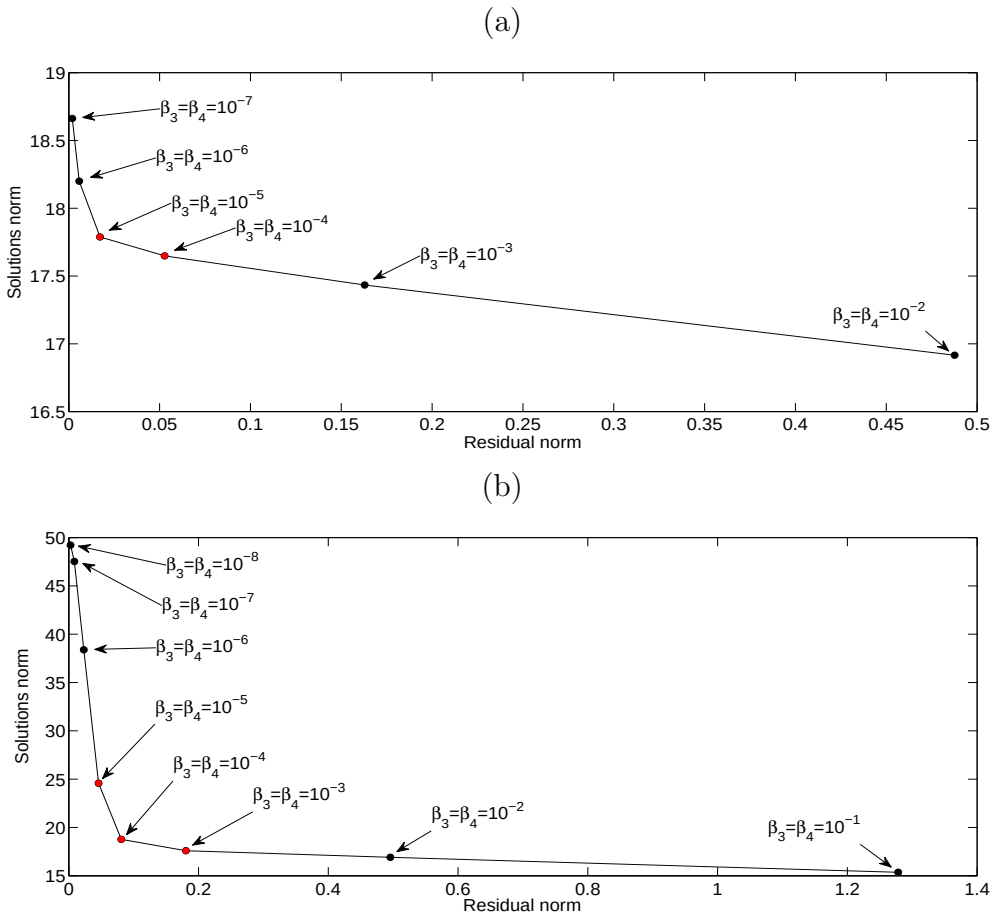

Figure 7: The residual norm versus the solution norm for various regularization parameters, for Example 1, with (a) $p = 0.01\%$ and (b) $p = 0.1\%$ noise.

(a)

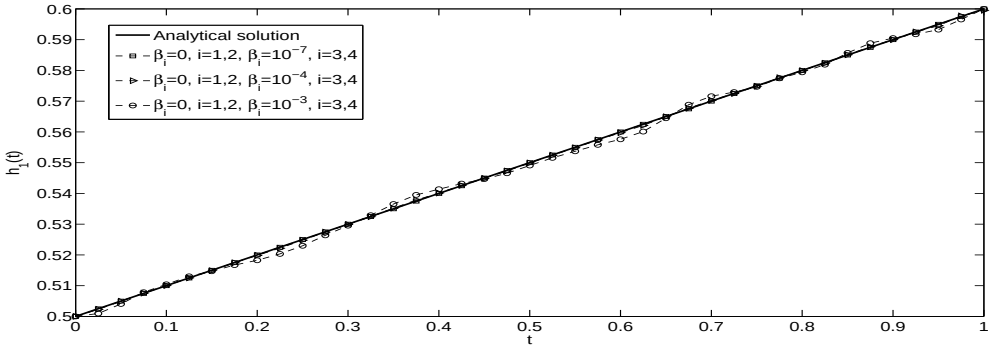

(b)

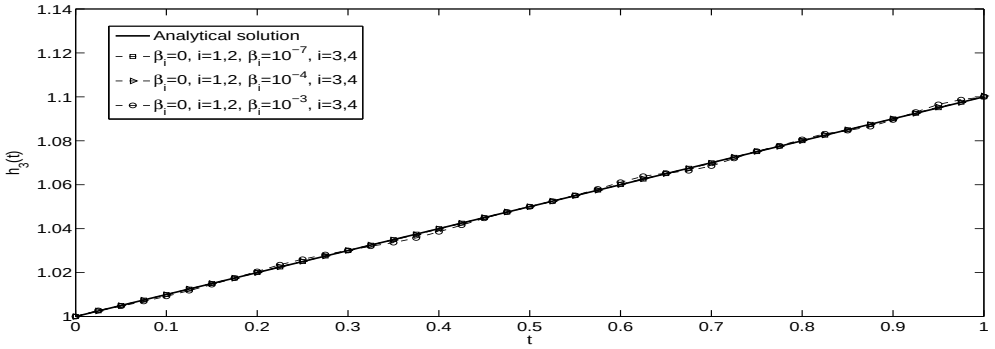

(c)

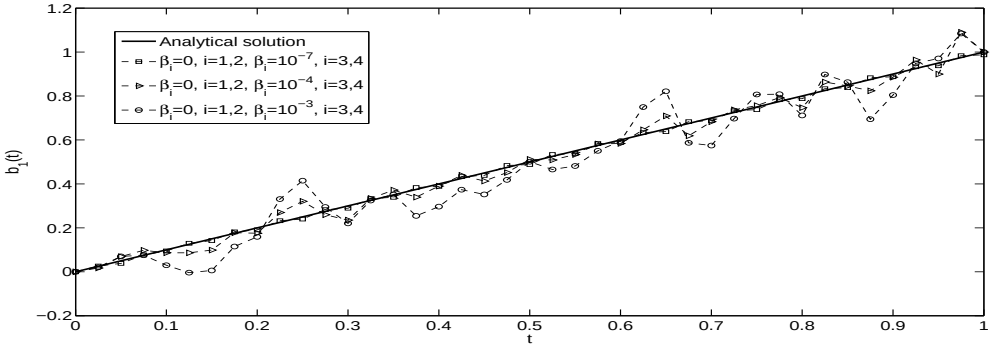

(d)

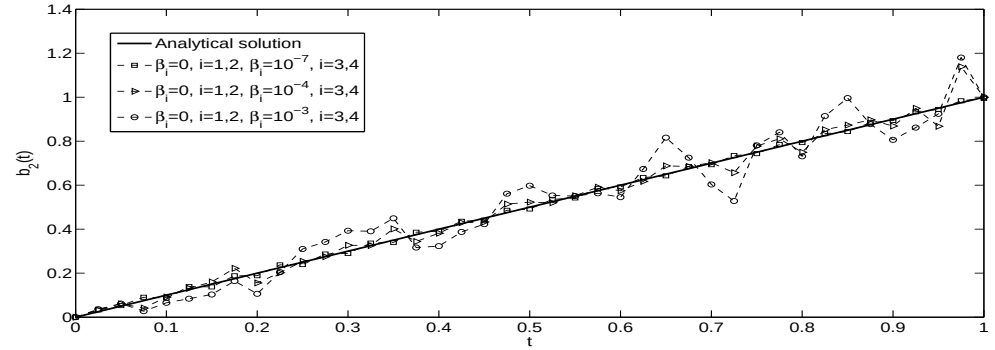

Figure 8: The analytical (45) and numerical solutions for: (a) $h_1(t)$, (b) $h_3(t)$, (c) $b_1(t)$ and (d) $b_2(t)$, for noise $p = 0$ $(-\square-)$, $p = 0.01\%$ $(-\triangleright-)$ and $p = 0.1\%$ $(-\circ-)$, with regularization, for Example 1.

5.2 Example 2 (for inverse problem II)

In this example, we consider the second inverse problem given by equations (1)–(3), (6), (7) and (21), with the same input data (40) and (42)–(46) as in Example 1, except that the data $\mu_3(t)$ and $\mu_4(t)$ given by equations (4) and (5) are replaced by the second and third-order heat moment $\mu_7(t)$ and $\mu_8(t)$ given by equations (22) and (23) as

$$\mu_7(t) = \frac{1+t}{3000}\Big(-1000 + 3250\pi - 250t + 1275\pi t - 15t^2 + 165\pi t^2 + 7\pi t^3 + (15+2t)^3 \tan^{-1}\Big(\frac{15+2t}{10}\Big) - (5+t)^3 \tan^{-1}\Big(\frac{5+t}{10}\Big) + 500 \ln\Big(\frac{325+60t+4t^2}{125+10t+t^2}\Big)\Big), \tag{48}$$

$$\mu_8(t) = \frac{1+t}{120000}\Big(5(10+t)(3\pi(20+3t)(50+t(14+t)) - 2(25+t(95+7t))) + 3(5+2t)(25+2t)(325+4t(15+t)) \tan^{-1}\Big(\frac{15+2t}{10}\Big) - 3(-5+t)(15+t)(125+t(10+t)) \tan^{-1}\Big(\frac{5+t}{10}\Big)\Big). \tag{49}$$

Table 1 shows that the analytical ((48) and (49)) and numerical solutions for $\mu_7(t)$ and $\mu_8(t)$ obtained with various mesh sizes $M = N \in \{10, 20, 40\}$ are in very good agreement.

One can remark that the conditions of Theorems 3 and 4 are satisfied and therefore, the local existence and uniqueness of the solution are guaranteed. The initial guesses for the vectors $\mathbf{h_1}$, $\mathbf{h_3}$, $\mathbf{b_1}$ and $\mathbf{b_2}$ are given by (47), the same as in Example 1. Note that the values of $b_1(0)$ and $b_2(0)$ are available from solving (24).

As we did in Example 1, we start the investigation with the case of exact input data (13), (14), (22) and (23), i.e. $p = 0$ in (37). The objective function F_1, as a function of the number of iterations without and with regularization is plotted in Figure 9.

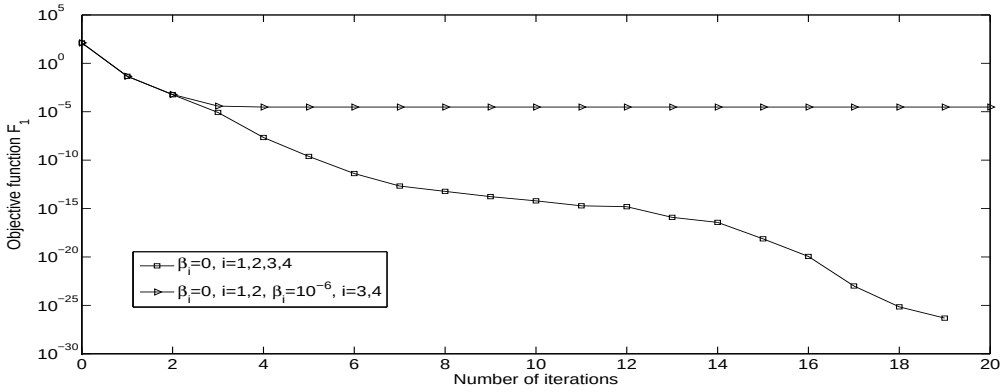

Figure 9: The objective function F_1, as a function of the number of iterations, no noise, with and without regularization, for Example 2.

From this figure, it can be seen that a monotonic convergence is rapidly achieved in a few iterations. The objective function F_1 decreases and takes a very low stationary

value of $O(10^{-27})$ in about 19 iterations when we do not employ any regularization, i.e. $\beta_i = 0$, $i = \overline{1,4}$, and of $O(10^{-5})$ in the case of regularization with $\beta_1 = \beta_2 = 0$, $\beta_3 = \beta_4 = 10^{-6}$. The numerical reconstruction results for the unknown coefficients are illustrated in Figure 10. From Figures 10(a) and 10(b) it can be noticed that very accurate recoveries for the free boundaries $h_1(t)$ and $h_3(t)$ are obtained. With no regularization, the numerical results for the coefficients $b_1(t)$ and $b_2(t)$ presented in Figures 10(c) and 10(d) are quite inaccurate with the values of $rmse(b_1) = 0.3001$ and $rmse(b_2) = 1.4094$, respectively. However, when we apply the regularization with $\beta_1 = \beta_2 = 0$, $\beta_3 = \beta_4 = 10^{-6}$ to F_1, we obtain more accurate reconstructions for $b_1(t)$ and $b_2(t)$, with $rmse(b_1)$ and $rmse(b_2)$ values decreasing to 0.0589 and 0.0498, respectively. Next, we consider the case of noisy data (13), (14), (22) and (23) perturbed by $p = 0.01\%$ noise, as in (38). We have also investigated higher amounts of noise p in (38), but the results obtained were less accurate and therefore, they are not presented. The investigation of the inversion of noisy data performed in this subsection, when compared with that of Example 1, indicates that the second inverse problem (1)–(3), (6), (7), (22) and (23) is more ill-posed than the first inverse problem (1)–(7).

The objective function F_1, as a function of the number of iterations, is shown in Figure 11. From this figure, it can be seen that in the case of no regularization, i.e. $\beta_i = 0, i = \overline{1,4}$, a slow convergence is recorded and, in fact, the process of minimization of the routine *lsqnonlin* is stopped when the prescribed maximum number of 400 iterations is reached. The corresponding numerical results for the unknown coefficients are presented in Figure 13.

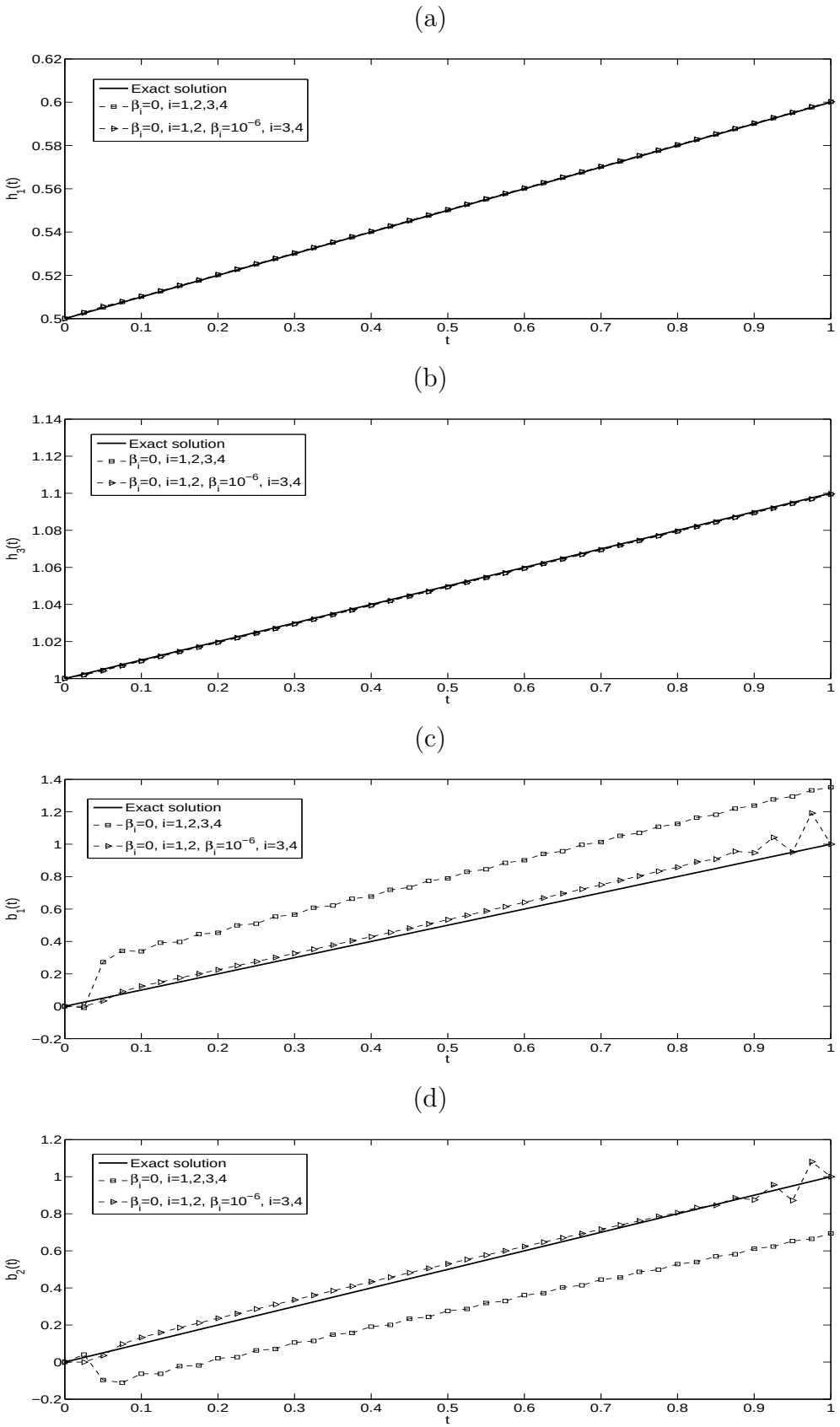

Figure 10: The analytical (45) and numerical solutions for: (a) $h_1(t)$, (b) $h_3(t)$, (c) $b_1(t)$ and (d) $b_2(t)$, no noise, with and without regularization, for Example 2.

From Figures 13(a) and 13(b) it can be seen that stable and accurate numerical results are obtained for the free boundaries $h_1(t)$ and $h_3(t)$. However, from Figures 13(c) and 13(d) one can observe that unstable (highly oscillatory) and very inaccurate solution for $b_1(t)$ and $b_2(t)$ are obtained with $rmse(b_1) = 48.1$ and $rmse(b_1) = 49.8$. This is expected since the problem under investigation is ill-posed and small errors in the input data (13), (14), (22) and (23) lead to a drastic amount of error in the output coefficients $b_1(t)$ and $b_2(t)$. Therefore, regularization is required in order to restore the stability of the solution in the coefficients $b_1(t)$ and $b_2(t)$.

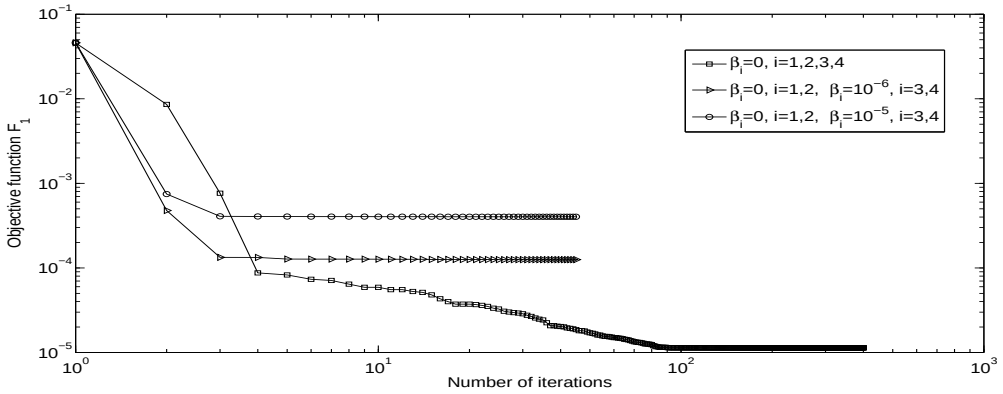

Figure 11: The objective function F_1, as a function of the number of iterations, for $p = 0.01\%$ noise, with and without regularization, for Example 2.

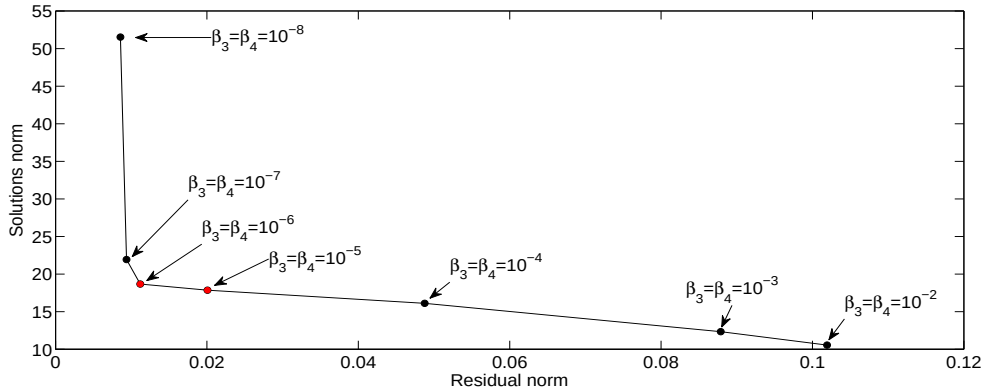

Figure 12: The residual norm versus the solution norm for various regularization parameters, for Example 2, with $p = 0.01\%$ noise.

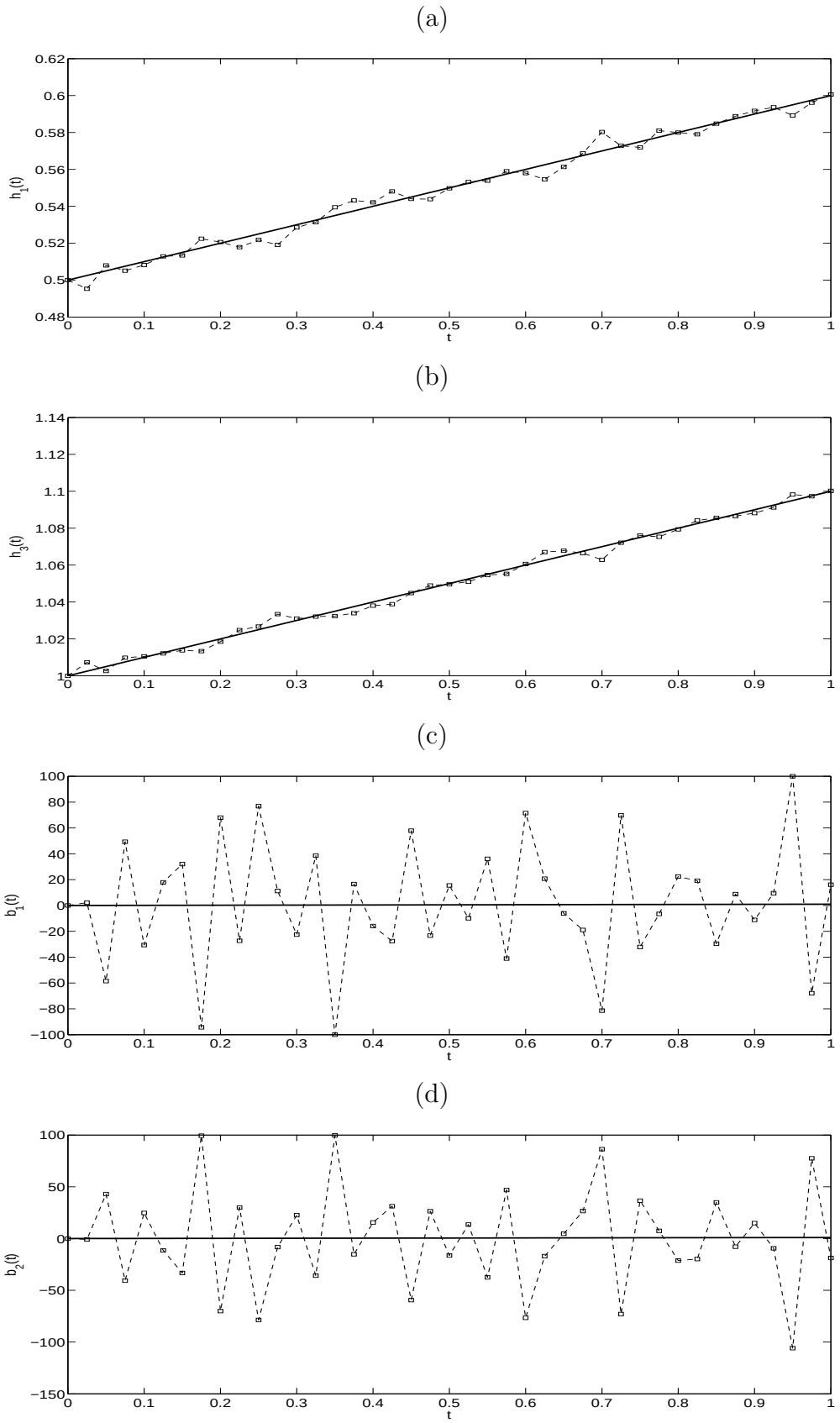

Figure 13: (
The analytical (—) and numerical solutions (−□−) for: (a) $h_1(t)$, (b) $h_3(t)$, (c) $b_1(t)$ and (d) $b_2(t)$, for ($p = 0.01\%$) noise, without regularization, for Example 2.)

(a)

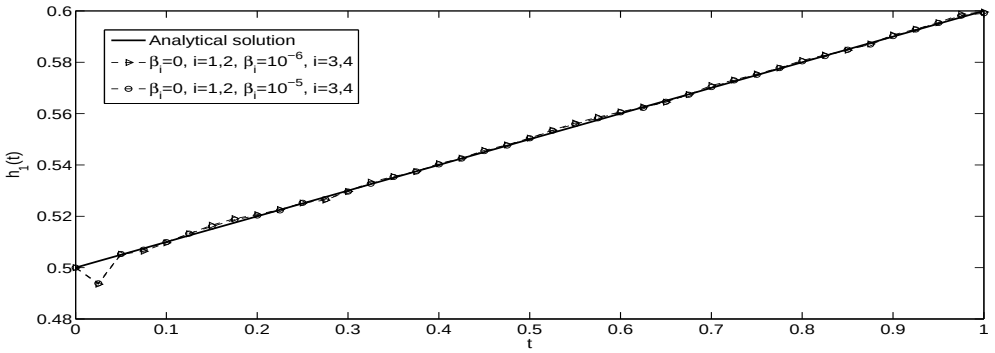

(b)

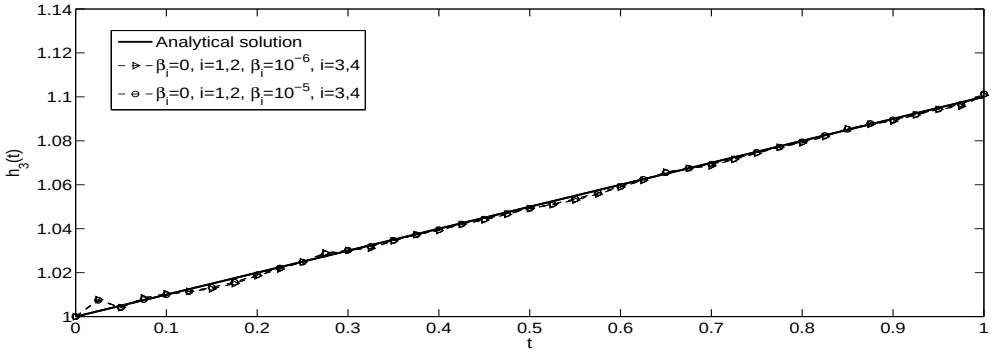

(c)

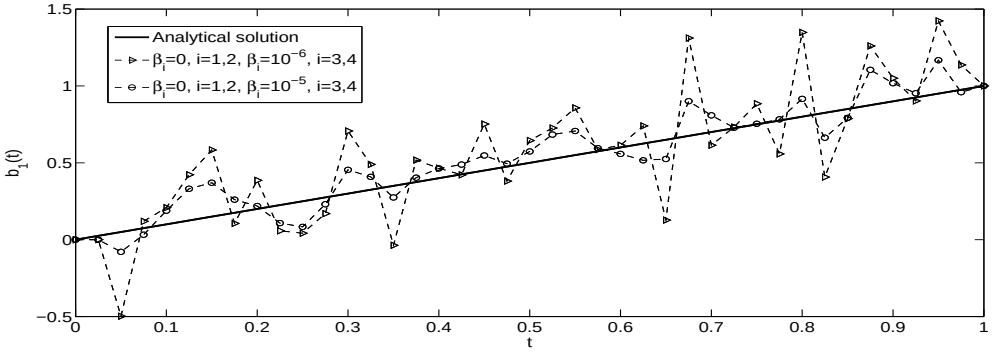

(d)

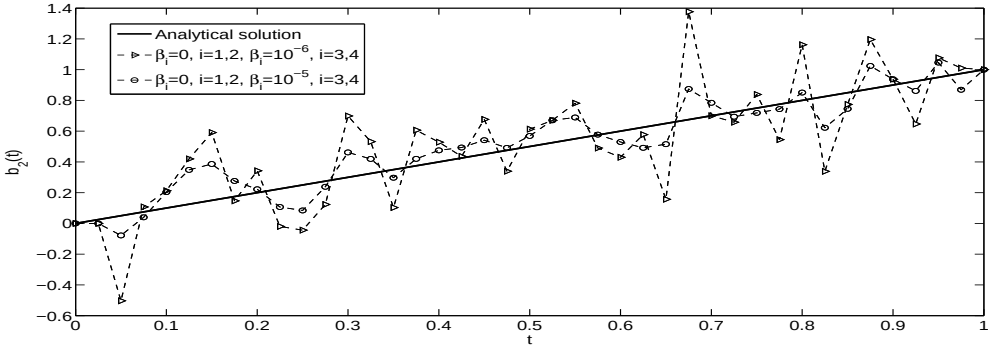

Figure 14: The analytical (45) and numerical solutions for: (a) $h_1(t)$, (b) $h_3(t)$, (c) $b_1(t)$ and (d) $b_2(t)$, for $p = 0.01\%$ noise, with regularization, for Example 2.

The L-curve, [8], for the choice of the regularization parameters is shown in Figure 12, by plotting the solution norm, as a function of the residual norm. From this figure, it can be observed that regularization parameters near the "corner" of the L-curve are $\beta_3 = \beta_4 \in \{10^{-6}, 10^{-5}\}$. The regularized decreasing monotonic convergence of the objective function F_1, as a function of the number of iterations, is shown in Figure 11. To stabilise the coefficients $b_1(t)$ and $b_2(t)$, we employ regularization with $\beta_3 = \beta_4 \in \{10^{-6}, 10^{-5}\}$ (suggested by the L-curve in Figure 12), obtaining $rmse(b_1) \in \{0.3062, 0.1594\}$ and $rmse(b_2) \in \{0.2920, 0.1590\}$, see Figures 14(c) and 14(d), for these coefficients. Furthermore, from Table 3 it can be seen that the computational time is reduced from 32 hours to 3 hours by the inclusion of regularization in F_1. For more, information about the $rmse$ values for $p = 0.01\%$ noise, with and without regularization, see Table 4.

Table 3: The $rmse$ values and computational time with $p = 0.01\%$ noise, for Example 2.

$\beta_i = 0, i = 1, 2$	$\beta_i = 0, i = 3, 4$	$\beta_i = 10^{-6}, i = 3, 4$	$\beta_i = 10^{-5}, i = 3, 4$
$rmse(h_1)$	3.9E-3	1.6E-3	1.4E-3
$rmse(h_3)$	2.6E-3	1.4E-3	1.1E-3
$rmse(b_1)$	48.1629	0.3062	0.1594
$rmse(b_2)$	49.8146	0.2920	0.1590
Computational time	32 hours	3 hours	3 hours

Table 4: The $rmse$ values for $p \in \{0, 0.01\%\}$ noise, with and without regularization, for Example 2.

p	Regularization	$rmse(h_1)$	$rmse(h_3)$	$rmse(b_1)$	$rmse(b_2)$
0	$\beta_i = 0, i = \overline{1,4}$	2.3E-4	5.2E-4	0.3001	1.4094
	$\beta_3 = \beta_4 = 10^{-8}$	2.8E-4	5.5E-4	0.1284	0.0729
	$\beta_3 = \beta_4 = 10^{-7}$	3.0E-4	5.6E-4	0.0620	0.0339
	$\beta_3 = \beta_4 = 10^{-6}$	**3.0E-4**	**5.4E-4**	**0.0589**	**0.0498**
	$\beta_3 = \beta_4 = 10^{-5}$	3.5E-4	4.2E-4	0.0739	0.0779
0.01%	$\beta_i = 0, i = \overline{1,4}$	3.9E-3	2.6E-3	48.1629	49.8146
	$\beta_3 = \beta_4 = 10^{-8}$	1.4E-3	1.4E-3	3.1935	3.2308
	$\beta_3 = \beta_4 = 10^{-7}$	1.5E-3	1.4E-3	0.7338	0.6982
	$\beta_3 = \beta_4 = 10^{-6}$	1.6E-3	1.4E-3	0.3062	0.2920
	$\beta_3 = \beta_4 = 10^{-5}$	**1.4E-3**	**1.1E-3**	**0.1594**	**0.1590**
	$\beta_3 = \beta_4 = 10^{-4}$	1.8E-3	1.9E-3	0.1632	0.1810
	$\beta_3 = \beta_4 = 10^{-3}$	5.0E-3	6.6E-3	0.4278	0.4377
	$\beta_3 = \beta_4 = 10^{-2}$	6.7E-3	8.9E-3	0.5657	0.5673
	$\beta_3 = \beta_4 = 10^{-1}$	6.9E-3	9.2E-3	0.5860	0.5858

6 Conclusions

A simultaneous determination of time-dependent coefficients and multiple free boundaries in the heat equation has been numerically investigated for the first time. The free boundary problems have been reduced to inverse coefficient problems in a fixed domain. The numerical solution of the direct problem based on the FDM with the Crank-Nicolson method has been employed. The inverse problem has been solved using the MATLAB optimisation toolbox routine *lsqnonlin* for minimizing the objective function F, or F_1. The Tikhonov regularization has been employed in order to obtain stable and accurate results because the inverse problem is ill-posed and very sensitive to noise. The numerical results have been presented and discussed for the two inverse problems, showing that accurate and stable approximate solutions have been achieved. Based on the numerical results and discussion we can conclude that the Stefan conditions (4) and (5) contain more information than the heat moments of several orders (22) and (23). Therefore, the second inverse problem (1)–(3), (6), (7), (22) and (23) is more ill-posed than the first inverse problem (1)–(7). Although not illustrated, similar conclusions have been obtained for other numerical tests concerning the recovery of non-smooth coefficients with multiple unknown free boundaries.

Acknowledgement

M.J. Huntul would like to acknowledge the finacial support received from Jazan University in Saudi Arabia and United Kingdom Saudi Arabian Cultural Bureau (UKSACB) in London for supporting his PhD at the University of Leeds.

References

[1] Broadbridge, P., Tritscher, P. and Avagliano, A. (1993) Free boundary problems with nonlinear diffusion, *Mathematical and Computer Modelling*, **18**, 15–34.

[2] Carrillo, J.A. and Vázquez, J.L. (2015) Some free boundary problems involving nonlocal diffusion and aggregation, *Philosophical Transactions of the Royal Society A*, **373**, 26261360.

[3] Caplan, M.E., Giri, A. and Hopkins, P.E. (2014) Analytical model for the effects of wetting on thermal boundary conductance across solid/classical liquid interfaces, *The Journal of Chemical Physics*, **140**, 154701.

[4] Chen, G.Q. and Feldman, M. (2015) Free boundary problems in shock reflection/diffraction and related transonic flow problems, *Philosophical Transactions of the Royal Society A*, **373**, 20140276.

[5] Coleman, T.F. and Li, Y. (1996) An interior trust region approach for nonlinear minimization subject to bounds, *SIAM Journal on Optimization*, **6**, 418–445.

[6] Friedman, A. (2015) Free boundary problems in biology, *Philosophical Transactions of the Royal Society A*, **373**, 20140368.

[7] Friedman, A. (2000) Free boundary problems in science and technology, *Notices of the American Mathematical Society*, **47**, 854-861.

[8] Hansen, P.C. (1992) Analysis of discrete ill-posed problems by means of the L-curve. *SIAM Review,* **34**, 561–580.

[9] Huntul, M.J., Lesnic, D. and Hussein, M.S. (2017) Reconstruction of time-dependent coefficients from heat moments, *Applied Mathematics and Computation*, **301**, 233–253.

[10] Huntul, M.J. and Lesnic, D. (2017) Time-dependent reaction coefficient identification problems with a free boundary, *Applied Mathematics and Computation*, submitted.

[11] Hussein, M.S., Lesnic, D., Ivanchov, M.I. and Snitko, H.A. (2016) Multiple time-dependent identification thermal problems with a free boundary, *Applied Numerical Mathematics*, **99**, 42–50.

[12] Hussein, M.S. and Lesnic, D. (2014) Determination of a time-dependent thermal diffusivity and free boundary in heat conduction, *International Communications in Heat and Mass Transfer*, **53**, 154–163.

[13] Hussein, M.S., Lesnic, D. and Ivanchov, M. (2013) Free boundary determination in nonlinear diffusion, *East Asian Journal on Applied Mathematics*, **3**, 295–310.

[14] Mathworks (2012) Documentation Optimization Toolbox-Least Squares (Model Fitting) Algorithms, available at www.mathworks.com/help/toolbox/optim/ug /brnoybu.html.

[15] Malyshev, I.G. (1975) Inverse problems for the heat-conduction equation in a domain with a moving boundary, *Ukrainian Mathematical Journal*, **27**, 568–572.

[16] Snitko, H.A. (2010) Coefficient inverse problem for a parabolic equation in a domain with free boundary, *Journal of Mathematical Science*, **167**, 30–46.

[17] Snitko, H.A. (2012) Inverse problem for determination of time-dependent coefficients of a parabolic equation in a free-boundary domain, *Journal of Mathematical Science*, **181**, 350–365.

[18] Snitko, G.A. (2014) On a coefficient inverse problem for a parabolic equation in a domain with free boundary, *Journal of Mathematical Sciences*, **200**, 374–388.

[19] Snitko, H.A. (2014) Inverse problem of finding time-dependent functions in the minor coefficient of a parabolic equation in the domain with free boundary, *Journal of Mathematical Science*, **203**, 40–54.

[20] Snitko, H.A. (2014) Determination of the lowest coefficient for a one-dimensional parabolic equation in a domain with free boundary, *Ukrainian Mathematical Journal*, **65**, 1698–1719.

[21] Smith, G.D. (1985) *Numerical Solution of Partial Differential Equations: Finite Difference Methods*, Clarendon Press, Oxford, Third edition.

M.J. Huntul[1,2],
[1]*Department of Applied Mathematics, University of Leeds,*
Leeds LS2 9JT, UK,
[2]*Department of Mathematics, Faculty of Science, Jazan University,*
P.O. Box 114, Jazan 45142, Saudi Arabia,
Email: mmmjmh@leeds.ac.uk
D. Lesnic[1],
[1]*Department of Applied Mathematics, University of Leeds,*
Leeds LS2 9JT, UK,
Email: amt5ld@maths.leeds.ac.uk

Received 21.06.2017, Accepted 26.06.2017